Ataxia and altered dendritic calcium signaling in mice carrying a targeted null mutation of the calbindin D28k gene

(calcium-binding protein/motor coordination/synaptically evoked calcium transients/cerebellar Purkinje neurons/calcium imaging)

Matti S. Airaksinen[*], Jens Eilers[†], Olga Garaschuk[†], Hans Thoenen[*], Arthur Konnerth[†], and Michael Meyer[*‡]

*Department of Neurochemistry, Max Planck Institute for Psychiatry, Am Klopferspitz 18A, D-82152 Martinsried, Germany; and †I. Physiologisches Institut, Universität des Saarlandes, D-66421 Homburg, Germany

ABSTRACT Intracellular calcium-binding proteins are abundantly expressed in many neuronal populations. Previous evidence suggests that calcium-binding proteins can modulate various neuronal properties, presumably by their action as calcium buffers. The importance of calcium-binding proteins for nervous system function in an intact integrated system is, however, less clear. To investigate the physiological role of a major endogenous calcium-binding protein, calbindin D28k (calbindin) *in vivo*, we have generated calbindin null mutant mice by gene targeting. Surprisingly, calbindin deficiency does not affect general parameters of development and behavior or the structure of the nervous system at the light microscopic level. Null mutants are, however, severely impaired in tests of motor coordination, suggesting functional deficits in cerebellar pathways. Purkinje neurons, the only efferent of the cerebellar cortex, and inferior olive neurons, the source of the climbing fiber afferent, have previously been shown to express calbindin. Correlated with this unusual type of ataxia, confocal calcium imaging of Purkinje cells in cerebellar slices revealed marked changes of synaptically evoked postsynaptic calcium transients. Their fast, but not their slow, decay component had larger amplitudes in null mutant than in wild-type mice. We conclude that endogenous calbindin is of crucial importance for integrated nervous system function.

Calbindin D28k is a member of a large family of intracellular calcium-binding proteins characterized structurally by EF-hand motifs (1, 2). It was originally purified from chicken intestine (3), and it is also expressed in kidney, where it is thought to facilitate transport of calcium across cells (4). Later, it was found to be expressed throughout the nervous system (5) in species ranging from invertebrates to mammals (6). In the mature nervous system, calbindin D28k expression is predominantly neuronal, and this protein has been found in long axon neurons, such as thalamic and striatonigral projection neurons, cerebellar Purkinje cells, and sensory neurons, and in short axon neurons, such as interneurons in the spinal cord, cerebral cortex, and hippocampus as well as dentate granule cells (1, 5, 7–10). Transient calbindin expression has been observed during embryonic development (11). Adult expression patterns develop steadily, as described in detail for the cerebellum (12). There, calbindin mRNA and protein increase postnatally to peak after the second postnatal week. In mature Purkinje cells, the major calbindin-expressing neuronal subtype in the cerebellum, calbindin contributes about 15% of total cellular

protein (8). Protein levels remain constant throughout most of the adult life span and decline in aged animals (13).

As demonstrated by overexpression or microinjection of calbindin in various cultured cell types (14, 15), calbindin can, by buffering calcium and by modulating calcium channel activity, regulate neuronal calcium homeostasis (16). Calcium buffers can modulate intracellular calcium transients by changing their time course and spatial spreading, and can thereby modify calcium-dependent intracellular signaling (17–21). Intrinsic neuronal firing patterns can depend on the presence of calbindin, as shown for supraoptic neurons in brain slices, where calbindin can switch firing modes from phasic to continuous (22). In addition, calbindin, when overexpressed, can modify synaptic interaction in hippocampal slices (23). Calcium-binding proteins have also been implicated as important regulators of neuronal degeneration in pathological processes (24, 25).

To facilitate analysis of the physiological roles of calbindin, we have created mice lacking calbindin by gene targeting. Calbindin-deficient mice develop surprisingly normally without apparent compensatory up-regulation of related calcium-binding proteins. However, when challenged in tests of movement coordination, severe ataxia is evident. Concomitant, synaptically evoked calcium transients in cerebellar Purkinje cells are strikingly altered.

MATERIALS AND METHODS

Gene Targeting. Calbindin genomic clones were isolated from a 129Sv library (Stratagene) using mouse calbindin cDNA (25) as a probe. A 10.3-kb *Hin*dIII–*Eco*RI fragment was used for the targeting vector. It was constructed by replacing a 1.3-kb *Cla*I–*Eco*47III fragment of the calbindin gene, containing part of the promoter and the first coding exon, with a 1.6-kb fragment containing the neomycin-resistance gene (*neo*) driven by the PGK promoter and bovine growth hormone polyadenylylation signal (26). R1 embryonic stem cells (27), grown on feeder cells with leukemia inhibitory factor, were electroporated and selected with G418 as described (28). Resistant clones were screened by Southern blot analysis using an external probe (see Fig. 1*A*) that recognizes a 7.8-kb wild-type band and a 5.5-kb mutant band after *Hin*dIII digestion and were identified at a 1/50 frequency. Additional integration of the vector was excluded by hybridization with a *neo* probe (data not shown). All five injected clones gave germline transmission, when the chimeras were crossed to C57BL/6 wild-type mice. Two lines (lines 1 and 15) derived from independent embryonic stem cell clones were used for the experiments. Littermates from heterozygote matings were used for all analyses.

Western Blot Analysis and Calcium-Overlay Assay. Supernatants of heat-treated (65°C) tissue homogenates of kidney,

‡To whom reprint requests should be addressed.

cerebellum, and brain without cerebellum, and protein standards (Swant, Bellinzona, Switzerland) underwent SDS/PAGE. The protein blots were stained with the following primary antibodies (all from Swant): mouse monoclonal antibodies against calbindin (300) and parvalbumin (235), rabbit polyclonal antisera against calbindin (CB38), calretinin (7696), parvalbumin (PV28), calbindin-D9k (CB9), calmodulin (465), and S100β (36). In addition, blots of postnuclear membrane fractions were stained with antibodies against the inositol 1,4,5-triphosphate receptor (29) and plasma membrane calcium pump (clone 5F10; Sigma). For detection, peroxidase-conjugated secondary antibodies (Boehringer Mannheim) and the enhanced chemiluminescence system (Amersham) were used. The calcium-overlay assay was done as described (30).

Histochemical Analysis. For immunostaining, mice were perfused with saline followed by 4% paraformaldehyde. Cryostat sections (40-μm thick) were stained free-floating with the primary antibodies referred to above, as well as with rabbit anti-PEP19 (31), and visualized using fluorescein-conjugated secondary antibodies (Jackson ImmunoResearch). Nissl and Golgi staining was done according to standard procedures.

Behavioral Analysis. All tests were performed on age-, sex-, and weight-matched animals by an experimenter blind to the genotype. The runway test was performed as described (32). Each day, each mouse underwent five consecutive trials. Slips were counted on one side. Drops were counted as follows: 0% in case of no drop or 100% in case of at least one drop. The stationary horizontal thin (1.5-cm diameter) rod test was done as described (32). The time an animal spent on the rod was measured; animals staying for 60 sec were taken from the rod and recorded as 60 sec. Three consecutive trials were performed. Gait analysis by footprinting (33) and grip strength measurements (28) were done as described.

Electrophysiology. Experiments were performed on Purkinje neurons in 200-μm-thick parasagittal cerebellar slices from 16- to 27-day-old mice as described (34) by an experimenter blind to the genotype. During the experiments, slices were perfused continuously with saline (30–33°C) containing 125 mM NaCl, 2.5 mM KCl, 2 mM CaCl$_2$, 1 mM MgCl$_2$, 1.25 mM NaH$_2$PO$_4$, 26 mM NaHCO$_3$, 20 mM glucose, and 0.01 mM bicuculline (Sigma), bubbled with 95% O$_2$ and 5% CO$_2$. The pipette solution contained 120 mM KCl, 10 mM Hepes, 10 mM

NaCl, 4 mM Mg-ATP, 0.4 mM Na-GTP, and 0.5 mM Calcium Green-1 (pH 7.3; Molecular Probes). Somatic tight-seal whole-cell recordings were obtained with pipettes that had an access resistance of 6–8 MΩ at the beginning of recording. At the time of fluorimetric measurements (restricted to a time window of 15–30 min after the start of the whole-cell recording), the access resistances were less than 14 MΩ. Synaptic stimulation of climbing fibers was as originally described (35).

Confocal Calcium Imaging. Calcium Green-1 fluorimetric calcium measurements were performed using a confocal laser-scanning system (Odyssey; Noran Instruments, Middleton, WI) mounted on an upright microscope (Axioplan; Zeiss) equipped with water immersion objectives (Achroplan; Zeiss; ×63, n.a. 0.9 and ×40, n.a. 0.75). The standard image acquisition rate was 30 Hz (60-Hz frame rate after off-line de-interlacing). All fluorescence data are background corrected and expressed as the increase in fluorescence divided by baseline fluorescence ($\Delta F/F$). Calcium transients after climbing fiber stimulation were systematically analyzed in dendritic branches of the Purkinje cell that were about 60–80 μm distant from the soma. The decay of all calcium transients was fitted with a biexponential function of time (t): $F(t) = Af \exp(-t/tf) + As \exp(-t/ts)$, where Af and As are the amplitudes, and tf and ts the time constants, of the fast and slow decay components, respectively.

Ratiometric fura-2 calcium measurements (see Fig. 4*F*) were performed as described (36, 37) using a variable scan, charge-coupled device imaging system (TILL Photonics, Planegg, Germany). For these experiments, 500 nM tetrodotoxin (Sigma) was added to the extracellular solution and the pipette solution contained 50 μM fura-2 instead of Calcium Green-1.

RESULTS

Mice Carrying a Targeted Disruption of the Calbindin Gene Develop Normally. To inactivate the calbindin gene, we replaced its promoter and first exon by a neomycin-resistance cassette (Fig. 1 *A* and *B*). Mutants were born at the expected Mendelian ratios, indicating that the calbindin mutation is not lethal to embryos. Mutant mice are not different from wild-type littermates with respect to growth, life span (the oldest being more than 1 one year old), and fertility, and all three
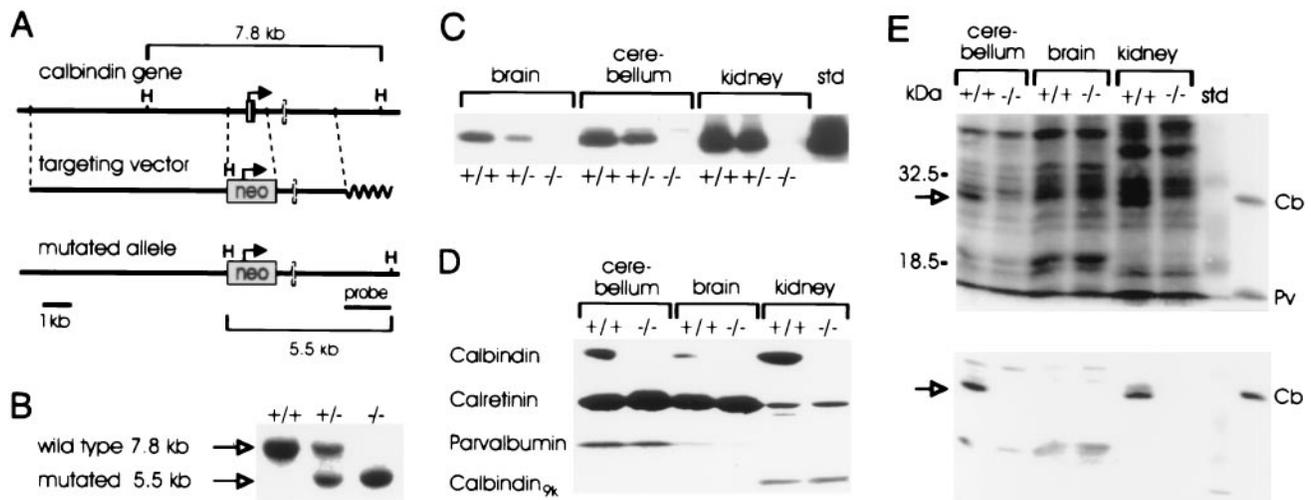

FIG. 1. Targeted disruption of the calbindin gene. (*A*) The targeting vector replaces part of the promoter and first exon with a *neo* cassette. H, *Hin*dIII. (*B*) Southern blot analysis of progeny from a heterozygote intercross. The 7.8- and 5.5-kb fragments indicate the wild-type and mutated alleles, respectively. (*C*) Calbindin protein is absent in homozygous and reduced in heterozygous mutant mice. (*D*) Western blot analysis of brain without cerebellum, cerebellum, and kidney of adult wild-type and mutant mice using a polyclonal calbindin antiserum. (*E*) Western blot analysis (*Upper*) and calcium-overlay assay (*Lower*) of adult cerebellum, brain without cerebellum, and kidney. Note the disappearance of the 28-kDa calbindin band (arrow) also in the Coomassie stained gel (*Upper*). Protein standards: Cb, calbindin; Pv, parvalbumin. +/+, Wild type; +/−, heterozygous; −/−, homozygous mutant.

genotypes are indistinguishable with respect to behavior in standard cage environments. Serum calcium and phosphate levels were within normal ranges (data not shown). To verify the null mutation, cerebellum, brain without cerebellum, and kidneys were analyzed by Western blotting and immunostaining using monoclonal and polyclonal antibodies against calbindin. No signals were detected in mice homozygous for the targeted mutation (Figs. 1*C* and 2 *C* and *D*), whereas reduced staining was observed in heterozygous mice (Fig. 1*C* and data not shown). Brain histology, as revealed by Nissl staining at 1 and 2 weeks, and 2 and 12 months of age, appeared normal (Fig. 2 *A* and *B* and data not shown).

Various Calcium-Binding Proteins Related to Calbindin Are Not Up-Regulated in Mutant Mice. To evaluate the possibility that the loss of calbindin is compensated for by up-regulation of its closest relative calretinin (38) or other members of the troponin-C superfamily of calcium-binding proteins (2), we analyzed lysates of cerebellum, brain without cerebellum, and kidney by Western blotting for calretinin, parvalbumin, and calbindin-D9k (Fig. 1*D*), as well as calmodulin and S100β (data not shown) and immunostained brain sections with antibodies against these proteins (Fig. 2 *F* and *G* and data not shown). No differences were observed between wild-type and mutant mice. Interestingly, this was also true for parvalbumin, another calcium-binding protein that is abundantly expressed in Purkinje cells (refs. 5 and 39; Figs. 1*D* and 2 *F* and *G*). In agreement with a published report (40), parvalbumin levels in brain without cerebellum were much lower than the levels in cerebellum. Moreover, calcium-overlay assays did not reveal up-regulation of any soluble, heat stable calcium-binding protein (Fig. 1*E Lower*). Calbindin was, however, clearly detected in wild-type kidney and cerebellum.
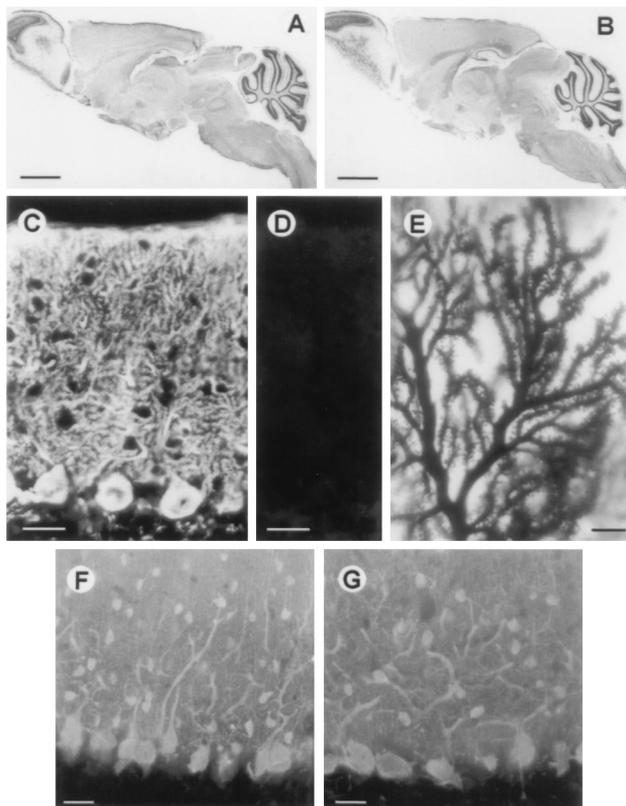

FIG. 2. Histological analysis. Midsagittal section of wild-type (*A*) and calbindin null mutant (*B*) mice stained with cresyl violet. Purkinje cells of wild-type (*C*) and null mutant (*D*) mice stained with antiserum to calbindin. (*E*) Golgi staining of Purkinje cell dendrites shows normal spine morphology and density. Purkinje cells of wild-type (*F*) and mutant (*G*) mice visualized with antiserum to parvalbumin.

Motor Coordination Is Impaired in Calbindin Null mutant Mice. As stated before, mutant and wild-type littermates were indistinguishable when observed in their normal cage environment. In addition, gait analysis by footprinting and grip strength measurement did not reveal differences (data not shown). When tested in the runway test, mutant animals were, however, severely impaired (Fig. 3). When placed on the runway, mutants, but not controls, displayed a shaky tremor that often became more intense during movement. The feet of mutants were slipping from the runway significantly more often than those of the wild-type littermate controls matched for weight and sex (Fig. 3*A*). In addition, 7-month-old mutants dropped from the runway in more than half of the first day trials (Fig. 3*B*). Controls never dropped. In contrast to slipping frequency, which was almost stable over the 4-day trial, the number of drops was decreased by about half on the second day and remained constant thereafter. Similar impairment was seen in null mutant lines derived from two independent embryonic stem cell clones (lines 1 and 15; Fig. 3 *A* and *B*). Wild-type animals from a pure 129Sv genetic background were not different from littermate controls (Fig. 3 *A* and *B*). Similar observations were made in older (10–12 months) animals (data not shown). The youngest age group tested consisted of 6-week-old males (Fig. 3*C*). Null mutants of this age almost never dropped, and compared with the older age groups, the number of slips was lower. As observed for older animals, consecutive sessions did not result in improvement of slipping. Fig. 3*C* also documents a clear gene dosage effect on runway performance. To gain more information on the development of the observed deficits, we tested an intermediate age group of 2-month-old males (data not shown). As reported for the 7-month-old group, these mutants dropped (about 50% of first day trials). The slipping rate for 2-month-old mice is similar to that of 7-month-old mice. Again, a clear gene dosage effect was observed (dat not shown).

As an additional test, 2-month-old animals were subjected to the thin horizontal stationary rod test (Fig. 3*C*). Clear deficits were observed for homozygous and heterozygous mutants over the first two sessions. Both types of mutants improved, and in the last session, significant differences were no longer observed. It should be noted that, in contrast to the runway task, the performance of the control group markedly improved in the rod test. Spontaneous tremor was never observed in any group.

Cerebellar Histology Is Apparently Normal in the Mutant Mice. The ataxia data prompted us to take a closer look at cerebellar physiology (see below) and histology. As demonstrated by parvalbumin (Fig. 2 *F* and *G*) and Golgi staining (Fig. 2*E*), the cerebellar Purkinje cell bodies and dendritic trees have normal morphology and spine density. Immunostaining for PEP19, another EF-hand protein expressed in Purkinje cells (31), did not differ between wild-type and mutant mice (data not shown). Nissl staining of cerebella from null mutant animals of different ages (1 week to 1 year) did not reveal any signs of degenerative changes within Purkinje cells (Fig. 2 *A* and *B* and data not shown). In addition, immunoblotting and immunostaining for the Purkinje cell marker's inositol trisphosphate receptor (29) and plasma membrane calcium pump (41) were similar in null mutant and wild-type animals (data not shown).

Synaptic Calcium Transients in Cerebellar Purkinje Neurons Are Strikingly Altered in Mutant Mice. For analysis of neuronal signaling, cerebellar slices of mutant and control mice were subjected to high resolution calcium imaging in combination with whole-cell patch clamp recordings. In wild-type animals, climbing fiber stimulation induced the well known electrical synaptic response ("complex spike"; ref. 42) associated with a postsynaptic calcium transient which was detected throughout the entire dendritic tree of the Purkinje cell (Fig. 4*A*; refs. 43 and 44). In null mutant mice, the complex
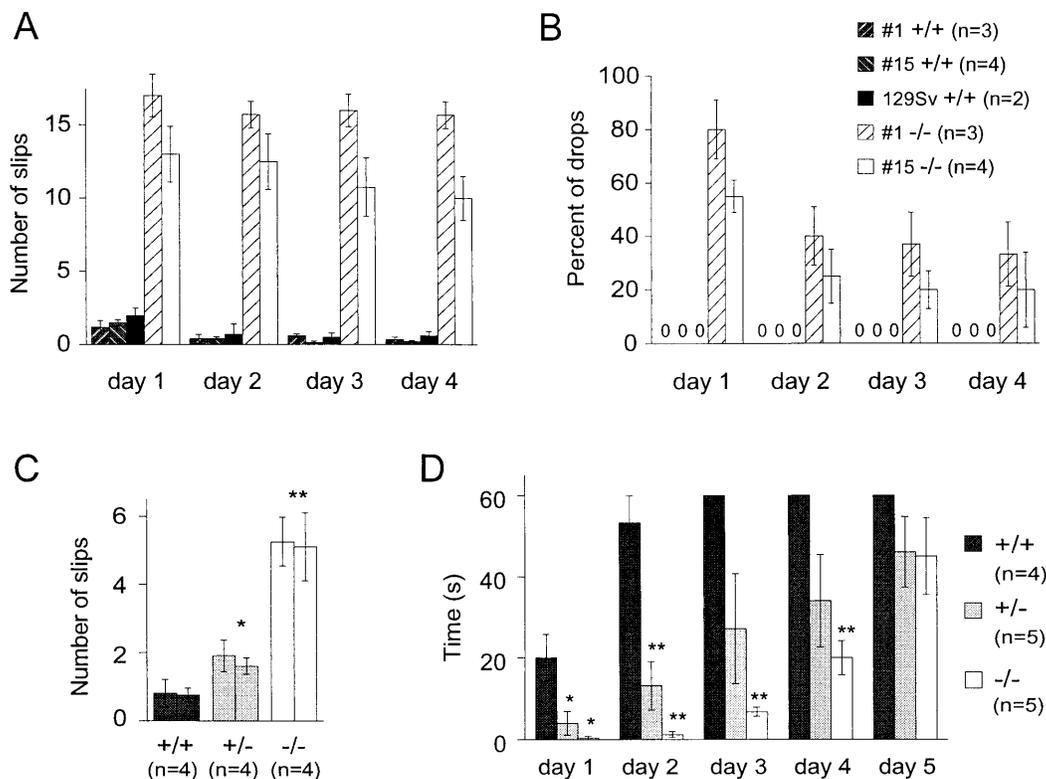
FIG. 3. Behavioral analysis. Performance of adult (7-month-old; *A* and *B*) and young adult (6-week-old; *C*) mice walking over a 1-m-long, 2-cm-wide runway. Four sessions on consecutive days are documented in *A* and *B*; the day 1 and 2 sessions after which no further changes were observed are shown in *C*. (*A*) Average number of slips counted on one side. (*B*) Percentage of drops during passage. In case of no drops, the value 0 is given at the position of the bar in *A*. Except for 129Sv mice (mean ± range), values are the means ± SEM. (*D*) Performance of 2-month-old males in the thin horizontal stationary rod test. The time spent on the rod up to a limit of 60 sec was measured. Values are the means ± SEM. *, $P < 0.05$; **, $P < 0.005$ compared with wild-type mice.

spikes (Fig. 4*B*) were similar to those registered in wild-type mice, rats (44), or other species (42, 45, 46). More specifically, in the mutant and the wild-type mice, single-shock climbing fiber electrical responses each consisted of a train of 4.9 ± 2.0 and 5.1 ± 1.6 spikes ($n = 7$ cells in 4 animals of each group, mean ± SEM), respectively. Moreover, the spiking frequency during complex spikes in null mutant and wild-type mice was 540 ± 105 and 505 ± 180 Hz, respectively, suggesting that under our experimental conditions, the firing properties of Purkinje cells were not significantly affected by the absence of calbindin. In contrast, dendritic calcium transients associated with complex spikes were profoundly altered in the mutant mice. Their peak amplitudes were enhanced on average by more than 80% [relative increase in fluorescence ($\Delta F/F$) was 0.44 ± 0.11 for wild-type and 0.80 ± 0.25 for null mutant littermates]. The decay of the calcium transients could be best fitted with a biexponential function (see *Materials and Methods*). We found that the values of the fast (*tf*) and the slow (*ts*) time constants were quite similar in wild-type (60 ± 10 msec and 720 ± 190 msec, $n = 6$ cells in 4 animals, for *tf* and *ts*, respectively) and null mutant (60 ± 20 msec and 780 ± 280 msec, $n = 7$ cells in 4 animals) mice. Similarly, the amplitude component *As* corresponding to *ts* did not differ significantly (Student's *t* test, $P > 0.05$) in wild-type (0.25 ± 0.08, $\Delta F/F$) and mutant (0.18 ± 0.07, $\Delta F/F$) mice. There was, however, a striking difference concerning the amplitude component *Af* (Fig. 4 *C–E*) that was found to be more than four times larger in the homozygous mutant mice than in control. The heterozygous mice were characterized by an intermediate mean value of *Af* (Fig. 4*E*), revealing a gene-dosage effect. Similar changes were observed for the calcium transients recorded in terminal spiny dendrites during the activation of subthreshold parallel-fiber- synaptic responses (34). As was the case for climbing

fiber stimulation, the parallel fiber-evoked calcium transient had a strikingly increased *Af* component in the calbindin-deficient mice (data not shown). Thus, calbindin controls the level of intracellular calcium within the first 100 msec following the calcium influx. It is noteworthy that in the cells dialyzed through the patch pipette, the difference in waveform of the transient was prominent in spite of the possible washout of some calbindin from control slices and in spite of possible saturation of the fluorescent dye in null mutant samples (47). Without these technical limitations, differences may be even larger. With an estimated dendritic dye concentration of about 350–400 μM (48), an association rate constant of about $0.9 \times 10^{-9} M^{-1} \cdot s^{-1}$ (49) and a K_d of about 220 nM (34) of Calcium Green-1 and a calbindin concentration in Purkinje cells of about 100–200 μM (8), calbindin apparently acts as a fast and high affinity calcium buffer. The resting calcium concentration was not changed (Fig. 4*F*).

DISCUSSION

The observation that calbindin null mutant mice develop normally without apparent signs of disturbed calcium metabolism suggests that calbindin expression in various peripheral organs (50) is either of minor importance for overall development or that its absence is compensated for by other mechanisms. Surprisingly, brain development also appeared normal. Although we used calcium-overlay assays and tested a panel of calcium-binding proteins without evidence for up-regulation, it is not possible to exclude partial compensation by untested or yet-unknown calcium-binding proteins. Further experiments were focused on the cerebellum, which contains high amounts of calbindin mainly in Purkinje cells. As for the brain, there was no evidence for up-regulation of calcium-
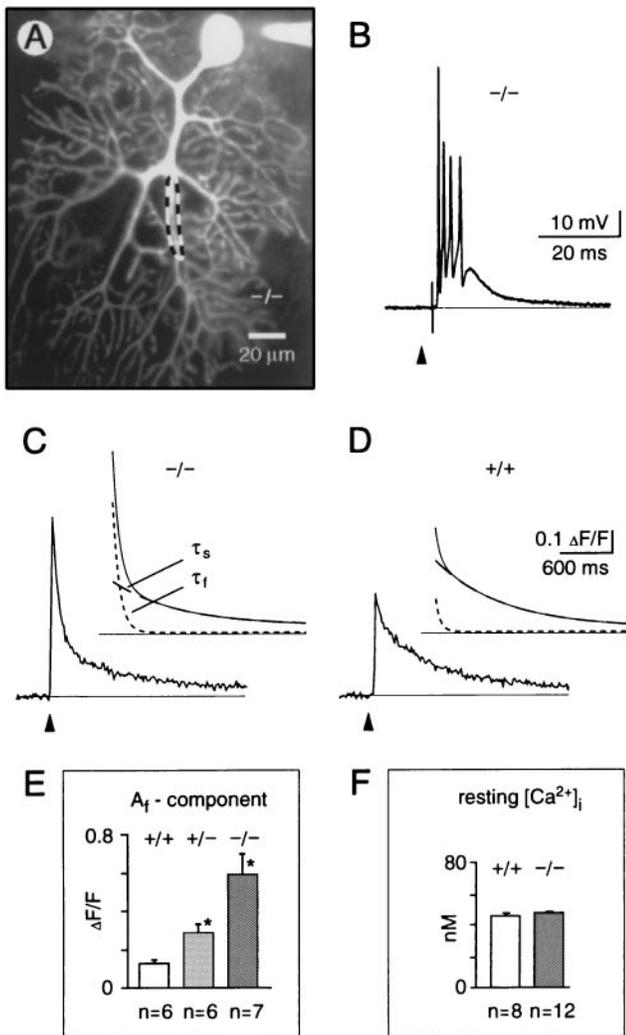
FIG. 4.   Synaptically evoked calcium transients in cerebellar Purkinje neurons from mice lacking calbindin. (*A*) Confocal fluorescence image of a Purkinje neuron in a cerebellar slice obtained from a 24-day-old null mutant mouse (−/−). The neuron was loaded through the recording patch pipette with the calcium indicator dye, Calcium Green-1. The region delimited by the dashed line indicates a typical dendritic area from which the fluorescence data (*C* and *D*) were obtained. (*B*) Excitatory postsynaptic potential (complex spike) evoked by extracellular stimulation of the afferent climbing fiber. Recording from a null mutant mouse, membrane potential (Vm) was −70 mV. (*C* and *D*) Dendritic calcium transients evoked by climbing fiber stimulation recorded in null mutant mice (*C*, −/−, average trace from $n = 7$ cells in 4 mice) and wild-type mice (*D*, +/+, average trace from $n = 6$ cells in 4 animals). The curves above each fluorescence trace represent superpositions of the corresponding double-exponential time-course fit (continuous line) with the fast (*tf*, dotted line) and the slow (*ts*, dashed line) components depicted separately. (*E*) *Af* amplitude components (corresponding to *tf*) of the synaptically induced calcium signals in wild-type, heterozygous (+/−) and null mutant mice, respectively. (*F*) Free intracellular calcium concentration ($[Ca^{2+}]_i$) under resting conditions measured in somata of fura-2 loaded cells (50 μM) of wild-type and null mutant mice. In *E* and *F*, values are the means ± SEM. The asterisk indicates significant difference to wild type (Student's *t* test, $P < 0.05$). Arrowheads mark the time points of single-shock synaptic stimulation.

binding proteins. It is, however, possible that the high levels of parvalbumin normally present in Purkinje cells (5, 39, 40) are sufficient to compensate partially for calbindin. Biochemical differences (50, 51) as well as different compartmentalization (39, 52–54) may all explain why both systems are not fully redundant. Double mutants lacking both calcium-binding proteins may provide further insights.

Previous studies targeting genes expressed in Purkinje cells (such as *mGluR1*, *PKCγ*, and *GluRδ2*) have shown that brain (presumably cerebellar) function can be markedly impaired in spite of normal light microscopic (e.g., refs. 32 and 55) and even electronmicroscopic (56) appearance. Ataxia and kinetic tremor present in calbindin mutants are typical signs of impaired cerebellar function (57). The fact that calbindin mutants are not ataxic in standard environments, such as those encountered in the cage or the footprint test, but display severely disturbed coordination only when challenged suggests impaired adaptation of automated compound movements to novel environmental requirements. Cerebellar function appears to be of crucial importance for these adaptation processes (58–60). The phenotype observed here is different from previous reports on GluRδ2 and PKCγ mutants (32, 33), which display ataxia already in standard environments. Interestingly, performance of calbindin mutants in a test not requiring walking (thin rod) was more significantly improved during consecutive training sessions than the movement related to slipping. This was found for all age groups. Possibly, malfunction of vestibular pathways that contain high calbindin levels (5) is responsible for initial failure in the balance test. Again, there are interesting but not readily interpretable differences in comparison to null mutants referred to above which did not improve on the thin bar (33). So far, our histological analysis does not provide an explanation for the age dependence of dropping. However, because all age groups were tested on the same equipment, a note of caution is necessary here.

Thus, the behavioral data are consistent with a major role of calbindin in cerebellar movement control. Altered signaling in Purkinje cells as well as presynaptic alterations in climbing fiber afferents that express calbindin in their soma (5) and axon terminals (61) need to be considered. Previous work suggests that inferior olive neurons may help organize movement (62) and are involved in motor adaptation (63). This has been proposed to require synchronization of neuronal ensembles which itself may be controlled by feedback from cerebellar nuclei (62). Thus, lack of calbindin may change the properties of this regulatory circuit at several places. Experimental activation of inferior olivary neurons by harmaline results in spontaneous tremor, presumably due to synchronization of inferior olive cells (64), indicating that generalized activation is unlikely to underlie the mutant phenotype. Destruction of part or all of the olive system by 3-acetyl-pyridine on the other hand results in pronounced ataxia (65).

On the cellular level, our results provide the first direct evidence that endogenous calcium-binding proteins critically control the waveform of synaptic calcium transients. Thus, our calcium imaging results extend previous studies in cultured cells (13, 14) in which increased levels of calbindin resulted in reduced peak amplitudes of slower calcium transients. Our data are best explained by assuming that calbindin acts as a fast, high affinity calcium buffer. A contribution of calcium extrusion mechanisms such as the plasma membrane calcium pump (41) seems to be less significant for regulating the fast synaptic component of the transient.

We can only speculate on the relation of the altered calcium transients and the change in phenotype. For example in Purkinje neurons, intracellular calcium signaling contributes to many cellular functions including (*i*) regular synaptic transmission by parallel (34) and climbing fibers (44), (*ii*) control of excitability (42, 66, 67), and (*iii*) induction of long-term changes in efficacy of excitatory (68) and inhibitory synapses (69). Thus, the impairment in motor coordination observed in the mutant mice may be the consequence of the malfunction of the regular patterns of cerebellar activity and/or deficits in learning and memorizing motor skills. Detailed *in vivo* and *in vitro* analyses as well as refined gene targeting approaches will

provide in the future useful means to identify the link between phenotype and the underlying cellular mechanisms.

1. Baimbridge, K. G., Celio, M. R. & Rogers, J. H. (1992) *Trends Neurosci.* **15,** 303–308.
2. Persechini, A., Moncrief, N. D. & Kretsinger, R. H. (1989) *Trends Neurosci.* **12,** 462–467.
3. Wasserman, R. H. & Taylor, A. N. (1966) *Science* **152,** 791–793.
4. Feher, J. J., Fullmer, C. & Wasserman, R. H. (1992) *Am. J. Physiol.* **262,** C517–C526.
5. Celio, M. R. (1990) *Neuroscience* **35,** 375–475.
6. Reifergerste, R., Grimm, S., Albert, S., Lipski, N., Heimback, G., Hofbauer, A., Pflugfelder, G. O., Quack, D., Reichmuth, C., Schug, B., Zinsmaier, K. E., Buchner, S. & Buchner, E. (1993) *J. Neurosci.* **13,** 2186–2198.
7. Jande, S. S., Maler, L. & Lawson, D. E. M. (1981) *Nature (London)* **297,** 765–767.
8. Baimbridge, K. G., Miller, J. J. & Parkes, C. O. (1982) *Brain Res.* **239,** 519–525.
9. Frantz, G. D. & Tobin, A. J. (1994) *J. Neurosci. Res.* **37,** 287–302.
10. Sequier, J. M., Hunziker, W., Andressen, C. & Celio, M. R. (1990) *Eur. J. Neurosci.* **2,** 1118–1126.
11. Andressen, C., Blümcke, I. & Celio, M. R. (1993) *Cell Tissue Res.* **271,** 181–208.
12. Iacopino, A. M., Rhoten, W. B. & Christakos, S. (1990) *Mol. Brain Res.* **8,** 283–290.
13. Lledo, P.-M., Somasundaram, B., Morton, A. J., Emson, P. C. & Mason, W. T. (1992) *Neuron* **9,** 943–954.
14. Chard, P. S., Bleakman, D., Christakos, S., Fullmer, C. S. & Miller, R. J. (1993) *J. Physiol.* **472,** 341–357.
15. Miller, R. J. (1991) *Prog. Neurobiol.* **37,** 255–285.
16. Albritton, N. L., Meyer, T. & Stryes, L. (1992) *Science* **258,** 1812–1815.
17. Sala, F. & Hernandez-Cruz, A. (1990) *Biophys. J.* **57,** 313–324.
18. Nowicky, M. C. & Pinter, M. J. (1993) *Biophys J.* **64,** 77–91.
19. Zhou, Z. & Neher, E. (1993) *J. Physiol.* **469,** 245–273.
20. Roberts, W. M. J. (1994) *J. Neurosci.* **14,** 3246–3262.
21. Li, Z., Decavel, C. & Hatton, G. I. (1995) *J. Physiol.* **488,** 601–608.
22. Chard, P. S., Jordan, J., Marcuccilli, C. J., Miller, R. J., Leiden, J. M., Roos, R. P. & Ghadge, G. D. (1995) *Proc. Natl. Acad. Sci. USA* **92,** 5144–5148.
23. Heizmann, C. W. & Braun, K. (1992) *Trends Neurosci.* **15,** 259–264.
24. Iacopino, A. M., Quintero, M. E. & Miller, E. K. (1994) *Neurodegeneration* **3,** 1–20.
25. Nordquist, D. T., Kozak, C. A. & Orr, H. T. (1988) *J. Neurosci.* **8,** 4780–4789.
26. Soriano, P., Montgomery, C., Geske, R. & Bradley, A. (1991) *Cell* **64,** 693–702.
27. Nagy, A., Rossant, J., Nagy, R., Abramow-Newerly, W. & Roder, J. C. (1993) *Proc. Natl. Acad. Sci. USA* **90,** 8424–8428.
28. Masu, Y., Wolf, E., Holtmann, B., Sendtner, M., Brem, G. & Thoenen, H. (1993) *Nature (London)* **365,** 27–32.
29. Mignery, G. A., Südhof, T. C., Takei, K. & De Camilli, P. (1989) *Nature (London)* **342,** 192–195.
30. Maruyama, K., Mikawa, T. & Ebashi, S. (1984) *J. Biochem.* **95,** 511–519.
31. Ziai, M., Pan, Y.-C. E., Hulmes, J. D., Sangameswaran, L. & Morgan, J. (1986) *Proc. Natl. Acad. Sci. USA* **83,** 8420–8423.
32. Kashiwabuchi, N., Ikeda, K., Araki, K., Hirano, T., Shibuki, K., Takayama, C., Inoue, Y., Kutsuwada, T., Yagi, T., Kang, Y., Aizawa, S. & Mishina, M. (1995) *Cell* **81,** 245–252.
33. Chen, C., Kano, M., Abeliovich, A., Chen, L., Bao, S., Kim, J. J., Hashimoto, K., Thompson, R. F. & Tonegawa, S. (1995) *Cell* **83,** 1233–1242.
34. Eilers, J., Augustine, G. J. & Konnerth, A. (1995) *Nature (London)* **373,** 155–158.
35. Konnerth, A., Llano, I. & Armstrong, C. M. (1990) *Proc. Natl. Acad. Sci. USA* **87,** 2662–2665.
36. Eilers, J., Schneggenburger, R. & Konnerth, A. (1995) in *Single Channel Recordings*, eds. Sakmann, B. & Neher, E. (Plenum, New York), pp. 213–229.
37. Garaschuk, O., Schneggenburger, R., Schirra, C., Tempia, F. & Konnerth, A. (1996) *J. Physiol.* **491,** 757–772.
38. Rogers, J. H. (1987) *J. Cell Biol.* **105,** 1343–1353.
39. Kosaka, T., Kosaka, K., Nakayama, T., Hunziker, W. & Heizmann, C. W. (1993) *Exp. Brain Res.* **93,** 483–491.
40. Endo, T., Takazawa, K., Kobayashi, S. & Onaya, T. (1986) *J. Neurochem.* **46,** 892–898.
41. de Talamoni, N. T., Smith, C. A., Wasserman, R. H., Beltramino, C., Fullmer, C. S. & Penniston, J. T. (1993) *Proc. Natl. Acad. Sci. USA* **90,** 11949–11953.
42. Llinas, R. & Sugimori, M. (1980) *J. Physiol.* **305,** 197–213.
43. Ross, W. N. & Werman, R. (1987) *J. Physiol.* **389,** 319–336.
44. Eilers, J., Callewaert, G., Armstrong, C. & Konnerth, A. (1995) *Proc. Natl. Acad. Sci. USA* **92,** 10272–10276.
45. Chan, C., Hounsgaard, J. & Midtgaard, J. (1989) *J. Physiol.* **409,** 143–156.
46. Miyakawa, H., Lev-Ram, V., Lasser-Ross, N. & Ross, W. N. (1992) *J. Neurophysiol.* **68,** 1178–1189.
47. Regehr, W. & Atluri, P. P. (1995) *Biophys. J.* **68,** 2156–2170.
48. Rexhausen, U. (1992) Diploma thesis (University of Göttingen, Göttingen, Germany), p. 66.
49. Eberhard, M. & Erne, P. (1991) *Biochem. Biophys. Res. Commun.* **180,** 209–215.
50. Christakos, S., Gabrielides, C. & Rhoten, W. B. (1989) *Endocr. Rev.* **10,** 3–26.
51. Leather, V. L. & Norman, A. W. (1993) *J. Cell. Biochem.* **52,** 243–252.
52. Feher, J. J. & Wasserman, R. H. (1979) *Biochim. Biophys. Acta* **585,** 599–610.
53. Winsky, L. & Kuznicki, J. (1995) *J. Neurochem.* **65,** 381–388.
54. Hubbard, M. J. & McHugh, N. J. (1995) *FEBS Lett.* **374,** 333–337.
55. Conquet, F., Bashir, Z. I., Davies, C. H., Daniel, H., Ferraguti, F., Bordi, F., Franz-Bacon, K., Reggiani, A., Matarese, V., Conde, F., Collingridge, G. L. & Crepel, F. (1994) *Nature (London)* **372,** 237–243.
56. Kano, M, Hashimoto, K., Chen, C. Abeliovich, A., Aiba, A., Kurihara, H., Watanabe, M., Inoue, Y. & Tonegawa, S. (1995) *Cell* **83,** 1223–1231.
57. Thompson, P. D. & Day, B. L. (1993) *Adv. Neurol.* **61,** 15–31.
58. Thach, W. T., Goodkin, H. P. & Keating, J. G. (1992) *Annu. Rev. Neurosci.* **15,** 403–442.
59. Llinas, R. & Welsh, J. P. (1993) *Curr. Opin. Neurobiol.* **3,** 958–965.
60. Raymond, J. L., Lisberger, S. G. & Mauk, M. D. (1996) *Science* **272,** 1126–1131.
61. Scotti, A. L. (1995) *J. Anat.* **187,** 649–659.
62. Welsh, J. P., Lang, E. J., Sugihara, I. & Llinas, R. (1995) *Nature (London)* **374,** 453–457.
63. Ojakangas, C. L. & Ebner, T. J. (1994) *J. Neurophysiol.* **72,** 2617–2630.
64. Llinas, R. & Volkind, R. A. (1973) *Exp. Brain Res.* **18,** 69–87.
65. Desclin, J. C. & Escubi, J. (1974) *Brain Res.* **77,** 349–364.
66. Hounsgaard, J. & Midtgaard, J. (1989) *J. Physiol.* **409,** 157–170.
67. Köhr, G., Lambert, C. E. & Mody, I. (1991) *Exp. Brain Res.* **85,** 543–551.
68. Konnerth, A., Dreessen, J. & Augustine, G. J. (1992) *Proc. Natl. Acad. Sci. USA* **89,** 7051–7055.
69. Kano, M., Rexhausen, U., Dreessen, J. & Konnerth, A. (1992) *Nature (London)* **356,** 601–604.